10-2021

The role of California sea lion (Zalophus californianus) hindflippers as aquatic control surfaces for maneuverability

Ariel M. Leahy

Frank E. Fish

Sarah J. Kerr

Jenifer A. Zeligs

Stefani Skrovan

See next page for additional authors

Authors

Ariel M. Leahy, Frank E. Fish, Sarah J. Kerr, Jenifer A. Zeligs, Stefani Skrovan, Kaitlyn L. Cardenas, and Megan C. Leftwich

© 2021. Published by The Company of Biologists Ltd | Journal of Experimental Biology (2021) 224, jeb243020. doi:10.1242/jeb.243020

RESEARCH ARTICLE

The role of California sea lion (*Zalophus californianus*) hindflippers as aquatic control surfaces for maneuverability

Ariel M. Leahy[1,*], Frank E. Fish[1], Sarah J. Kerr[1], Jenifer A. Zeligs[2], Stefani Skrovan[2], Kaitlyn L. Cardenas[1] and Megan C. Leftwich[3]

ABSTRACT

California sea lions (*Zalophus californianus*) are a highly maneuverable species of marine mammal. During uninterrupted, rectilinear swimming, sea lions oscillate their foreflippers to propel themselves forward without aid from the collapsed hindflippers, which are passively trailed. During maneuvers such as turning and leaping (porpoising), the hindflippers are spread into a delta-wing configuration. There is little information defining the role of otarrid hindflippers as aquatic control surfaces. To examine *Z. californianus* hindflippers during maneuvering, trained sea lions were video recorded underwater through viewing windows performing porpoising behaviors and banking turns. Porpoising by a trained sea lion was compared with sea lions executing the maneuver in the wild. Anatomical points of reference (ankle and hindflipper tip) were digitized from videos to analyze various performance metrics and define the use of the hindflippers. During a porpoising bout, the hindflippers were considered to generate lift when surfacing with a mean angle of attack of 14.6±6.3 deg. However, while performing banked 180 deg turns, the mean angle of attack of the hindflippers was 28.3±7.3 deg, and greater by another 8-12 deg for the maximum 20% of cases. The delta-wing morphology of the hindflippers may be advantageous at high angles of attack to prevent stalling during high-performance maneuvers. Lift generated by the delta-shaped hindflippers, in concert with their position far from the center of gravity, would make these appendages effective aquatic control surfaces for executing rapid turning maneuvers.

KEY WORDS: Biomechanics, Turning, Hindflippers, Delta wing, Porpoising

INTRODUCTION

The fundamental challenges of locomotion in the marine environment are vastly different from those experienced in the terrestrial environment. Most marine mammals are essentially neutrally buoyant underwater (Fish, 2004) and therefore do not have to support themselves against gravity to swim. However, the aquatic environment presents marine mammals with a unique set of challenges including the balance between stability (i.e. steady movement along a predictable trajectory) and maneuverability (i.e. the rate of change in movement or trajectory) and the total energetic cost of locomotion (Williams et al., 2000; Williams, 2001; Fish, 2002).

Stability and maneuverability are controlled by both passive and active elements (Fish, 2002; Fish and Lauder, 2017). The passive elements refer to the animal's morphology, whereby the shape of the animal and its control surfaces (i.e. surfaces used for propulsion or maneuvering) affect stability/maneuverability. The active elements refer to the neuromuscular and musculoskeletal manipulation of control surfaces by expending energy (Fish, 2002; Fish and Lauder, 2017). According to Fish's (2002) arrow model, there are six conditions that promote stability: (1) the center of gravity is located anteriorly, (2) control surfaces are affixed far from the center of gravity, (3) the majority of control surfaces are located at the posterior position of the body, (4) control surfaces exhibit both sweep (i.e. rearward sloping of the leading edge) and dihedral (i.e. tilting towards the body), (5) control surfaces express limited mobility, and (6) the body has limited flexibility (Fish, 2002; 2004). The morphology of sea lions (Genus: *Zalophus*) deviates from all these conditions, indicating these animals are highly maneuverable. However, this has only been examined in depth for the California sea lion (*Zalophus californianus*) (Feldkamp, 1987b; Fish et al., 2003; Fish, 2004). It is important to note that with the accessibility of *Z. californianus* both in the wild and in captivity, this singular species has come to represent its entire taxonomic family (Otariidae) with respect to the morphologic and biomechanic literature.

Indeed, sea lion bodies are highly flexible and the flippers so highly mobile that these animals can adduct both the hindflippers and foreflippers into a position where the body is completely free of control surfaces. In such body positions, corresponding instabilities are utilized to accomplish highly acrobatic maneuvers such as rolling or somersaulting by dorsal bending (Fish et al., 2003). These animals complete more typical maneuvering behaviors, such as turning and leaping from the water onto land, with a high degree of agility as well (Fish et al., 2003). The unstable morphology of *Z. californianus* enhances this maneuvering capacity and affects their heightened turning performance (Fish et al., 2003).

Sea lions propel themselves underwater with the use of their foreflippers. This reliance on the foreflippers is different from most marine mammals, which produce thrust with the caudal portion of their body. Thus, most studies on *Z. californianus* swimming mechanics and maneuverability have focused on the role of the foreflippers (English, 1976; Godfrey, 1985; Feldkamp, 1987a; Fish et al., 2003; Friedman and Leftwich, 2014). During normal, rectilinear swimming, sea lions swim by use of foreflipper 'flapping', capitalizing on both lift- and drag-based systems, while the hindflippers trail behind with the digits adducted, reducing drag forces on the body (Gordon, 1983; English, 1976; Feldkamp, 1987a). During turning maneuvers, the wing-like foreflippers are abducted and held statically through the turn, creating a centripetal force on the foreflippers (Godfrey, 1985; Fish et al., 2003). The

[1]West Chester University, West Chester, PA 19383, USA. [2]SLEWTHS, Animal Training & Research International, Moss Landing, CA 95039, USA. [3]George Washington University, Washington, DC 20052, USA.

*Author for correspondence (al916349@wcupa.edu)

A.M.L., 0000-0002-7790-197X

Received 14 June 2021; Accepted 3 September 2021

Journal of Experimental Biology (2021) 224, jeb243020. doi:10.1242/jeb.243020

location of the foreflippers close to the sea lion's center of gravity dampens the effects of this force and there is no evidence that the foreflippers are held at an angle that quantifies sufficient lift production to accomplish the turn (Fish et al., 2003; Fish, 2004). This presents the question of where the primary forces are acting on the body to complete these maneuvers.

The hindflippers during aquatic maneuvering behaviors have been largely overlooked. Anatomically, the position of the hindflippers, well posterior of the center of gravity, presents the potential to create ample torque through lift generation (Fish et al., 2003). The hindflippers have previously been described to operate as rudders (Tarasoff, 1972; Godfrey, 1985; Fish et al., 2003), but the mechanics behind this assertion have not been determined. Godfrey (1985) also described the hindflippers as functioning similar to the tail of a bird, which could prove essential in executing tight turns and other high-performance maneuvers.

Subaqueous turns can be divided into two main categories based on the animal's propulsion throughout the turn. During powered turns, animals continuously propel themselves through the turn. During unpowered turns, animals cease all thrust production and simply glide through the turn (Fish, 2002). Animals performing powered turns are able to maintain or increase speed and acceleration once the turn is completed, but these turns have generally larger radii than unpowered turns (Fish, 2002). Sea lions mainly perform sharp, banking, unpowered turns. *Zalophus californianus* initiates and determines turn direction by dorsal bending of the spine (Godfrey, 1985; Fish et al., 2003). Dorsal bending continues as the sea lion coordinates foreflipper abduction with a 90 deg roll of the body, while abducting the hindflippers (Godfrey, 1985; Fish et al., 2003) (Fig. 1). While gliding through the unpowered turn, the sea lion's body rotation and hydrofoil-shaped foreflippers create a centripetal force, while the hindflippers steady the posterior of the body to allow the abdominopelvic areas to follow the curved path of the turn (Godfrey, 1985; Fish et al., 2003; Fish, 2004).

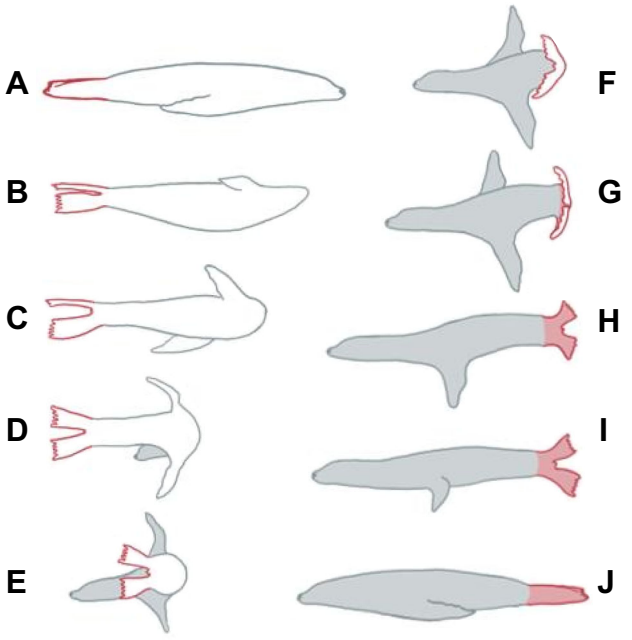

Fig. 1. Visual depiction of a California sea lion (*Zalophus californianus*) performing a left 180 deg banking turn. (A–J) The sequence runs top left to bottom right. The hindflippers are highlighted in red, and the shaded portion of the sea lion represents the portion of the animal that has completed the turn. Figure adapted from Godfrey (1985) and provided with permission from S. Godfrey.

Porpoising is the serial leaping and submerged swimming behavior thought to reduce transport costs for numerous air-breathing marine species such as porpoises, dolphins, sea lions and penguins (Au and Weihs, 1980; Hui, 1987; Blake and Smith, 1988; Fish and Hui, 1991; Yoda et al., 1999). This behavior involves an upward change in trajectory from submerged swimming to aerial flight. Investigations into the potential benefits (e.g. energy economy, speed, respiration) of porpoising have only been completed for dolphin and penguin species (Au and Weihs, 1980; Hui, 1987; Blake and Smith, 1988; Fish and Hui, 1991). However, the benefits of porpoising found in other air-breathing marine vertebrates may apply to *Zalophus* (Boness, 2009). Porpoising behaviors require the use of control surfaces (e.g. fins or flippers) to generate a lift force to produce an upward (positive) pitch to the body in order to send the animal across the air-water interface.

As aforementioned, biological control surfaces aid in stabilization, propulsion and/or maneuverability (Fish, 2002; Fish and Lauder, 2017). A subset of these control surfaces is referred to as biological delta-wings. In aerodynamics, delta-wings are recognized for their triangular shape and ability to maintain lift at high angles of attack (i.e. angle with respect to flow) and delay stall, or loss of lift (Polhamus, 1966; Marchman, 1981; Katz and Plotkin, 1991; Rom, 1992; Thompson, 1992; Hamizi and Khan, 2019). In biology, delta-shaped control surfaces have convergently evolved in various vertebrate clades. Biological delta-wings differ from true delta-wings as the presence of a body and limbs connected to the delta-shaped control surface alters lift properties; however, the benefits through lift generation are still evident (Evans, 2003). Anatomically, the hindflippers of *Zalophus* possess a strong triangular morphology resembling a delta-shape. Depending on the angle at which the hindflippers are utilized during aquatic maneuvering, the hindflippers may function as biological delta-wings, offering large surfaces for lift production.

The hindflippers of sea lions, in concert with the propulsive foreflippers, may act as passive control surfaces during aquatic maneuvers, such as turning and porpoising. As the position of the sea lion's foreflippers are positioned near the center of mass (Fish, 2002), the foreflippers by themselves may not generate sufficient centripetal acceleration to perform a tight turn (Fish, 2004). However, the posterior position of the delta-shaped hindflippers and the angle at which the hindflippers are held may provide sufficient torque and lift to execute high-performance maneuvers. With respect to aquatic locomotion and maneuverability, the hindflipper mechanics of sea lions have not previously been investigated. Thus, the primary goal of this study was to determine whether sea lion hindflippers operate as aquatic control surfaces to gain insight into lift-based aquatic maneuverability. We hypothesized that a sea lion's hindflippers function as essential aquatic control surfaces, more specifically as biological delta-wings, which generate the lift force that allows sea lions to successfully porpoise and complete tight turns at high speeds.

MATERIALS AND METHODS

Digital video analysis

Sea lion, *Zalophus californianus* (Lesson 1828), porpoising and bank turning were digitally analyzed from video to identify the functions of the hindflippers during each behavior. This research was performed under West Chester University IACUC 201601.

Journal of Experimental Biology (2021) 224, jeb243020. doi:10.1242/jeb.243020

Porpoising

Captive porpoising behavior was video recorded at the National Zoo of the Smithsonian Institution in Washington, DC, USA. The sea lion enclosure at the National Zoo provided a viewing platform with combined underwater and above-water views. One adult female sea lion (1.45 m) was trained to porpoise in its 1,135,623 l saltwater enclosure in front of and parallel to the plane of a 5 m long, 2.5 m high viewing window. Two Canon EOS 5D Mark III cameras were positioned on tripods in the front-center of the viewing window, with one camera positioned to capture the underwater view, and the other camera, directly above, positioned to capture the leap above the surface of the water. Natural light was sufficient to illuminate the viewing window. Prior to the recording session, a recording was made of a linear scale (0.5 m) centrally positioned on the outside of the viewing window at the level of the air–water interface. However, as the leaps of the sea lion varied in distance from the viewing window, the known body length (BL) of the animal, measured from the tip of the nose to the tip of the tail, was used as a relative scale. Video of each porpoising bout was recorded at 60 frames s^{-1}. We restricted our analyses to strictly the aerial or submerged phase of individual porpoising leaps and analyzed that phase from the respective above- and below-water views to reduce error due to refraction across the air–water interface. Porpoising analyses were completed using a combination of Tracker software (v.5.1.3: https://physlets.org/tracker/) and ImageJ (v.1.52a, NIH).

In Tracker, anatomical points of reference including the nose, tip of the foreflipper, ankle and tip of the hindflipper nearest the viewing window were digitized to visualize the path of locomotion as well as calculate values for water exit/escape velocity (m s^{-1}) (Table 1). Water exit velocity was defined as the velocity of the animal's nose as it approached the surface of the water just prior to breaking the surface. The video frame in which the sea lion's nose crossed the water–air boundary was identified, then the video was backtracked six frames. Porpoising exit velocity was calculated as the displacement of the sea lion's nose over the five frames prior to breaking the surface of the water, divided by the elapsed time. Similarly, water escape velocity was the velocity of the nose just after the animal broke the surface of the water and initiated the aerial phase of the leap, thus escaping the water. Porpoising escape velocity was calculated as the displacement of the sea lion's nose over five frames, after it broke the surface of the water, divided by the elapsed time.

The same anatomical points of reference were analyzed in ImageJ to measure the leap height and length (BL), the exit/entry angles of the sea lions before/after the leap, as well as the angle of attack of the hindflippers during the submerged portion of the porpoising behavior (Table 1). For exit/entry angle, the fifth video frame post-surface break was utilized. One line was drawn from the tip of the sea lion's nose, through the midline of the head/neck, and the other was drawn across the surface of the water. The porpoising exit/entry angle was measured as the angle between these two lines. In total, 29 individual leaps from this single sea lion were analyzed.

Porpoising leaps were recorded in the field for wild sea lions in Monterey Bay, CA, USA. Video recordings at 30 frames s^{-1} were captured with an iPhone6, mounted on a tripod, from the R/V *John H. Martin*, a 17.1 m long vessel. The ocean condition was a sea state of 1 (calm). The porpoising motion was analyzed from videos of the sea lion as the trajectory of their leaps was perpendicular to the camera. The aerial phase of 106 porpoising leaps was similarly analyzed with a combination of Tracker software and ImageJ. The relative BL was measured in ImageJ as the length down the midline from the tip of the nose to the tip of the tail representing 1 BL. Vertical height of the leap relative to BL and exit angle were also measured (Table 1).

Turning

Banked turning was recorded at SLEWTHS in Moss Landing, CA, USA. A clear acrylic window (1 m×0.5 m) was affixed with four foam sides to create a floating surface viewing box to reduce surface distortion during the trials. Two volunteers held the viewing box with the acrylic side facing down, on the surface of the water by the edge of a 1.22 m deep, 4.57 m×7.32 m saltwater pool for each turning trial. A Canon EOS 5D Mark III camera was mounted on a ladder above the acrylic viewing box to film directly down into the water at 60 frames s^{-1}.

Three adult sea lions (two females and one male – F_1: 1.96 m, F_2: 1.82 m, M_1: 2.24 m) were trained to perform a 180 deg banked left turn directly under the viewing box. Prior to the recording session, a recording was made of a linear scale (0.5 m) resting inside the viewing box. In total, 86 individual banking turns were recorded, 70 of which (F_1: 30, F_2: 28, M_1: 12) were found to be acceptable for video analysis. Turning sequences were deemed unusable if the sea lion did not complete the turn under the viewing box, or if the animal came in contact with the viewing box during the turn, which caused the accumulation of bubbles under the box and reduced visibility. For recordings of each individual turn, anatomical points of reference (nose, right and left ankle joints, and right and left hindflipper tips) were digitized throughout the path of the turn.

Calculations

The positions of reference points for each video frame during a turning maneuver were put into a custom-written Matlab code to calculate the turning rate (ω; deg s^{-1}) and the turning radius (r; m) (Table 1). The turning rate, converted into radians s^{-1}, and radius were used to calculate turning velocity ($\mathbf{U}$; m s^{-1}), by:

$$\mathbf{U} = \omega \times r. \quad (1)$$

Table 1. Maneuverability variables measured for each behavior, location and specimen

Captive porpoising		Wild porpoising		Captive turning		Flipper specimen	
Variable	Units	Variable	Units	Variable	Units	Variable	Units
Exit velocity	m s^{-1}	Exit angle	deg	Turning rate (ω)	deg s^{-1}	Spread angle	deg
Escape velocity	m s^{-1}	Leap length	BL	Turning radius (r)	m and %BL		
Exit angle	deg	Leap height	BL	Turning velocity ($\mathbf{U}$)	m s^{-1}		
Entry angle	deg			Centripetal acceleration (a_c)	m s^{-2} and $\boldsymbol{g}$		
Leap length	BL			Angle of attack (α)	deg		
Leap height	BL						
Angle of attack (α)	deg						

Journal of Experimental Biology (2021) 224, jeb243020. doi:10.1242/jeb.243020

Centripetal acceleration (a_c; m s^{-2}) in multiples of gravitational acceleration ($\boldsymbol{g}$; 9.81 m s^{-2}) was calculated as:

$$a_c = \frac{\mathbf{U}^2}{r\,\boldsymbol{g}}. \quad (2)$$

Angle of attack (α) is a measurement of angle with respect to flow. Especially in captive aquatic environments, where there is a lack of currents, the best representation of flow is the trajectory of the maneuvering animal. For measurements of angle of attack of the hindflippers during porpoising and banked turns, sequential video frames of the tracked ankle joints and hindflipper tips were analyzed in ImageJ according to Fish et al. (1988), where the ankle joints were used to visualize the trajectory of the animal and representative flow. In this method, angle of attack is measured as the angle between one line drawn from the tip of the hindflipper through the ankle joint, and the other drawn from the tip of the hindflipper to its location in the following frame. For porpoising, angle of attack was measured on the hindflipper closest to the viewing window during the submerged, lift-producing phase of the behavior and then averaged for that leap. For bank turning, several precautions were taken to reduce error in the 2D measurements of this rotationally complex behavior. First, angle of attack was measured for the right and left hindflippers independently of one another to account for potential variance caused by the positioning of the hindflippers at different depths. Second, this measurement was only taken during the 0.3–0.5 s period where the animal remained fully banked and the hindflippers were fully visible under the viewing window. Third, angle of attack was only taken if the frontal plane of the hindflipper remained vertically oriented throughout the turn. Angling of the hindflippers in any way that exposed more than the medial or lateral edge of the flipper disqualified that hindflipper from angle of attack measurements. All the qualified angles of attack measured for an individual hindflipper during a banked turn were averaged for that turn.

Shape analysis

As the video data collected in this study was 2D and filmed from lateral views, the delta-morphology of the hindflippers during porpoising and turning could not be analyzed from video. Instead, the spread angle of five hindflipper specimens was measured. *Zalophus californianus* hindflippers were acquired from the Marine Mammal Center in Sausalito, CA, USA. The hindflippers were a code 2 on the decomposition scale (i.e. a fresh carcass) and were extracted from adult male and female carcasses (Pugliares et al., 2007). All flippers were stored at −20°C and were completely thawed just prior to examination. Using a Cannon EOS 5D Mark III camera, thawed hindflippers were photographed from above in an abducted posture to represent the flipper during maneuvering. Spread angle was assessed in ImageJ (v.1.52a, NIH) by drawing a line along the center of the first and last digits to the flipper base and measuring the angle between the two (Table 1).

Statistical analysis

All statistical analyses were performed using Microsoft Excel (2010) or SPSS (v.24.0). Statistical analyses for the porpoising behaviors were limited because of the sample size of one animal. Means±1 s.d. were calculated using data from 29 individual leaps. Unfortunately, the unbalanced nature of the bank turning dataset, as a result of small sample size (n=3) and other constraints, disallowed the use of an ANOVA model to determine differences in bank turning between individuals and across control surfaces. Alternatively, means and 95% confidence intervals were reported (Di Stefano, 2004) for each of the turning variables and for the extreme 20% of the data. Paired t-tests were used to determine differences of the hindflippers within individuals and unpaired t-tests for differences between male and females. Additionally, regression equations and correlation coefficients were used to investigate the relationship between turning variables. In all statistical tests, P<0.05 was considered significant (Whitlock and Schluter, 2015).

RESULTS

Porpoising

Under trainer control, the sea lion executed a series of porpoising leaps (Movie 1). A total of 29 leaps were analyzed. Porpoising leaps progressed along a wave-like path of crests (i.e. peak of the aerial leap) and troughs (i.e. lowest submerged point). The cycle of a single porpoising leap was analyzed from crest to crest. The sea lion was completely airborne in all leaps. While fully aerial, the sea lion displayed convex curvature of the body, with the foreflippers adducted flush against the underside of the abdomen, or venter of the body, and the digits of the hindflippers fully spread or abducted. Water entry was initiated with the nose and the body followed in a curved trajectory. On entry into the water, the foreflippers supinated and remained swept along the lateral torso as the anterior third of the sea lion became submerged. When the remaining two-thirds of the animal entered the water, the sea lion abducted its foreflippers and dorsally flexed its spine. The digits of the hindflippers remained abducted through water entry and stabilized the posterior region to the bottom trough of the sea lion's submerged trajectory, where the animal would then simultaneously pitch up with its head and adduct the foreflippers until perpendicular to the body. In this submerged phase, the sea lion followed a parabolic trajectory, keeping the digits of the hindflippers abducted, while both pronating and retracting the foreflippers until flush with the venter of the body just prior to exiting the water. The animal continued on this trajectory until fully aerial at the crest of the leap (Fig. 2).

The duration of a full cycle of porpoising from water entry to water entry for the single sea lion was 1.5±0.11 s. When comparing the velocity of the sea lion's submerged approach to the surface (exit velocity) to its velocity after breaking the surface of the water (escape velocity), the animal's velocity was reduced by an average of 57.3% while crossing the water–air interface (Table 2). The sea lion leapt out of the water at high angles, ranging from 60 to 82 deg (Table 2). Despite this exaggerated exit angle, the sea lion's

Table 2. Maximum and minimum values for porpoising leap performance and angle of attack of the hindflippers through the submerged lift-producing phase calculated from a single captive female sea lion

	Exit velocity (m s^{-1})	Escape velocity (m s^{-1})	Exit angle (deg)	Entry angle (deg)	Leap length (BL)	Leap height (BL)	Angle of attack (deg)
Mean±s.d.	2.13±0.26	1.22±0.24	70.0±6.3	37.8±6.9	0.83±0.14	0.37±0.08	14.6±6.3
Maximum	2.66	1.76	82.2	57.3	1.05	0.52	18.3
Minimum	1.71	0.86	60.0	28.7	0.61	0.23	10.8

Means±s.d. of each measurement are also provided.

Journal of Experimental Biology (2021) 224, jeb243020. doi:10.1242/jeb.243020

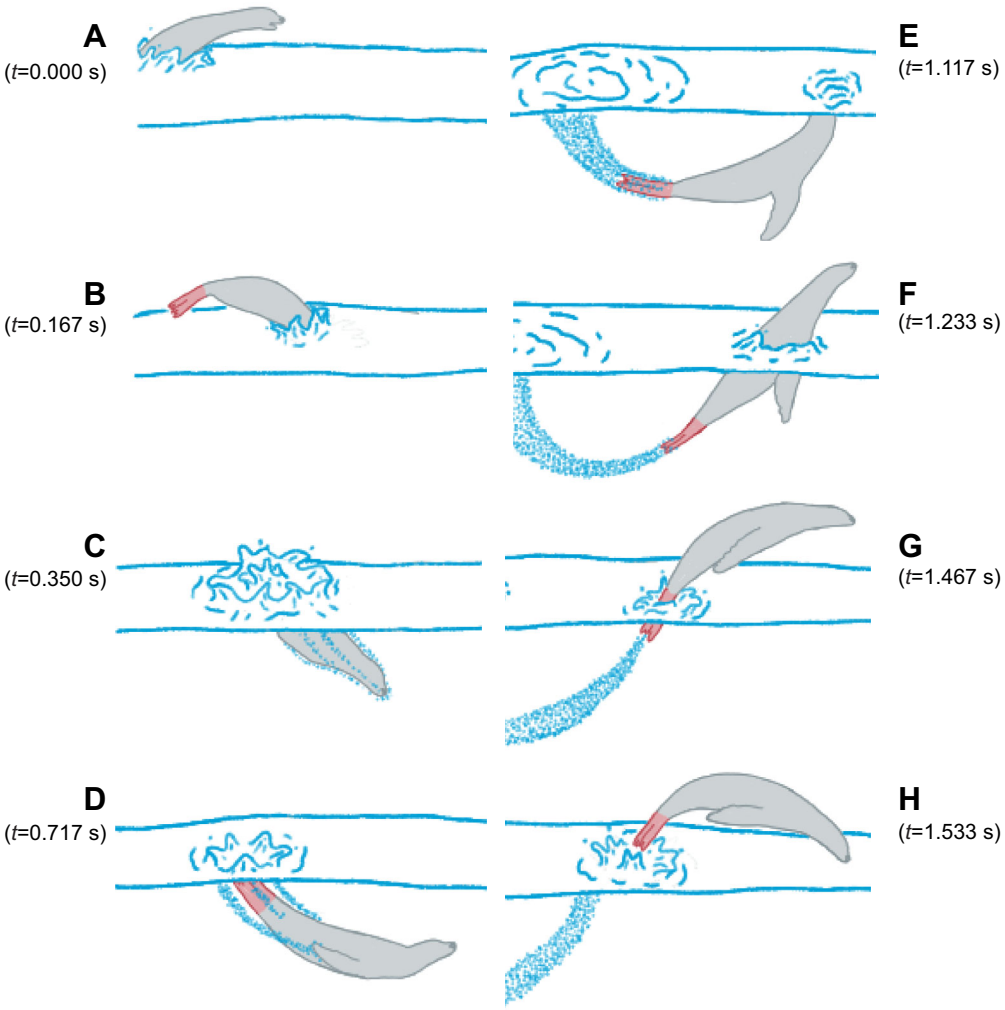

Fig. 2. Artistic rendition of a captive female California sea lion completing one porpoising leap. (A–H) The porpoising sequence, with corresponding times (*t*), runs from top left to bottom right, beginning with the animal to the left of the frame, out of the water. The red coloration highlights the hindflippers.

porpoising leaps were on average 2.2 times longer than they were high (Table 2). The angle of attack of the hindflippers during the submerged lift-producing phase of the behavior ranged from 10.8 to 18.3 deg (Fig. 2D–F, Table 2).

Porpoising was displayed by wild sea lions in Monterey Bay in groups of 12 to over 100 individuals (Movie 2). A total of 106 individual leaps were analyzed. Leaps ranged from only the head and body in the air to the whole animal being airborne with the nose and tip of the hindflippers clearing the surface of the water. During the aerial phase of the leap, the head and posterior of the body were flexed, giving the body a convex appearance. Leap length was 0.81 ±0.06 BL. The exit angle was 45.6±7.2 deg. The vertical height attained during the leap was 0.26±0.05 BL. The leap length of the wild sea lions was approximately equivalent to the leaps of the trained sea lion, but the exit angle and leap height of the wild sea lions were 35% and 30% lower than those of the trained sea lion, respectively.

Turning

The sea lions in this study only performed left 180 deg banked turns (Movie 3) with a total of 70 turning sequences analyzed. Starting at the opposite end of the pool, the sea lions initiated an acceleration and swam nose first toward the experimental area under the viewing box, with the foreflippers adducted against the venter of the body and the hindflippers adducted. A banked turn was initiated by lateral flexion of the neck toward the direction of the turn, followed by a simultaneous near-90 deg counterclockwise roll of the body, abduction of the foreflippers, and abduction of the hindflippers, which expanded the interdigital webbing and increased the surface area of the hindflippers (Fig. 3). The animals held all their flippers in this configuration while dorsally arching the spine until the 180 deg turn was approximately 75% complete. From this point, the sea lions adducted, pronated and retracted the foreflippers flush against the venter of the body. As the turn was completed, the animal

Table 3. Maximum and minimum values for bank turning performance about the hindflippers for captive male and female California sea lions

	Maximum Ω (deg s^{-1})	Minimum *r* (m)	Minimum *r* (BL)	Maximum **U** (m s^{-1})	Maximum a_c (m s^{-2})	Maximum a_c (***g***)	Maximum α (deg)
Females	644.4	0.27	14.3	3.8	37.6	3.8	50.8
20% extreme	540.7±34.6	0.30±0.02	15.9±0.01	3.3±0.22	30.8±3.4	3.1±0.4	40.9±3.8
Male	386.7	0.31	10.9	2.6	14.1	1.4	48.5
20% extreme	353.2±57.0	0.34±0.07	13.4±0.02	2.27±0.25	12.2±2.2	1.3±0.2	36.2±8.2

Means±s.d. for the 20% extremes of each variable are also provided. Data are for 2 females and 1 male.

Journal of Experimental Biology (2021) 224, jeb243020. doi:10.1242/jeb.243020

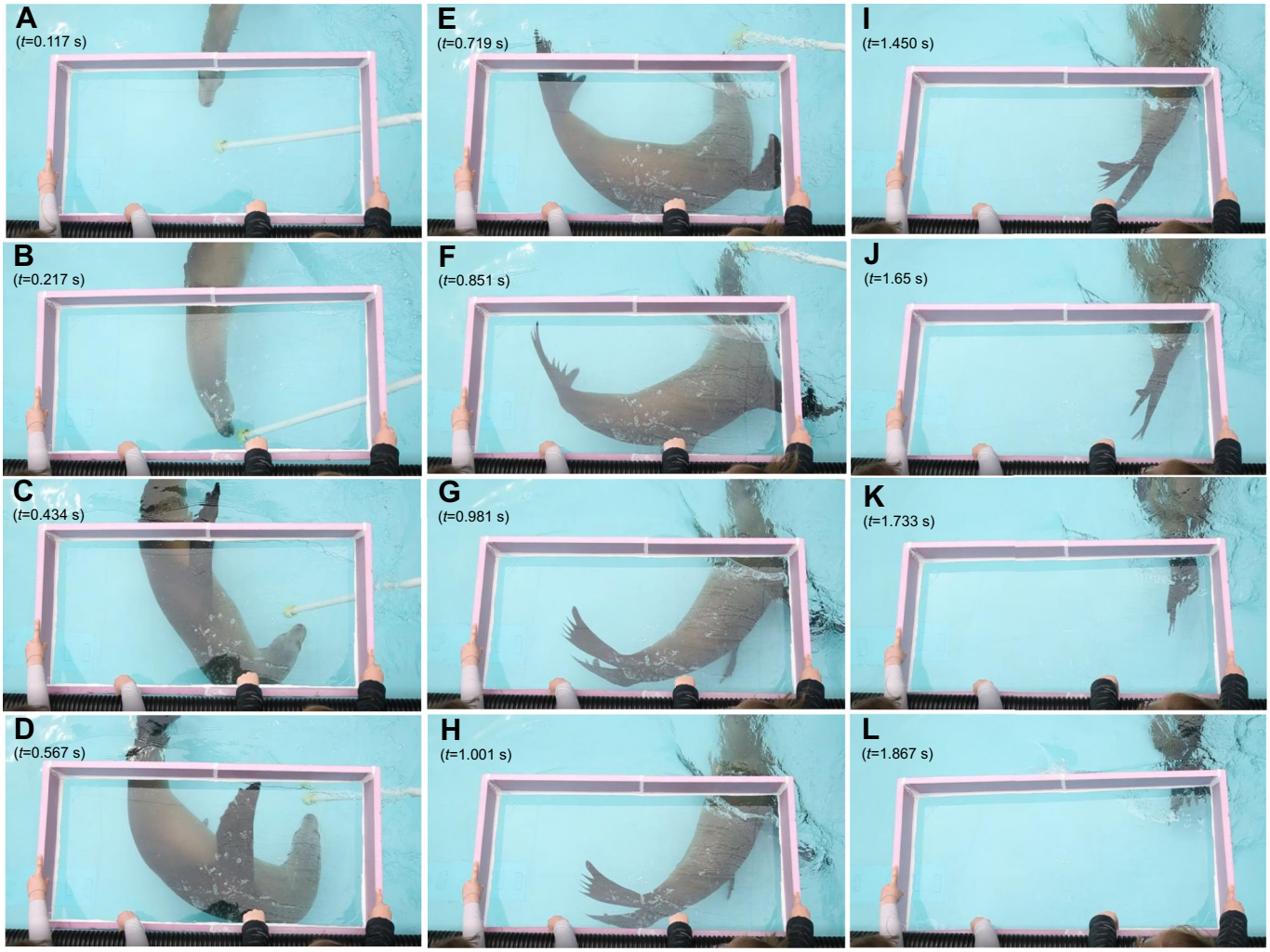

Fig. 3. Series of images from video of a captive female California sea lion completing a left 180 deg banking turn as viewed from above, through an acrylic viewing box. (A–L) The turning sequence, with associated times (*t*), runs from top left to bottom right. The target pole (PVC pole with tennis ball on the end) used to direct the sea lion through the turn is visible in images A–F.

straightened its body and simultaneously reversed the 90 deg roll. The digits of the hindflippers remained in an abducted posture until the turn was finished, at which point the sea lion performed a foreflipper stroke to propel itself back to its starting position at the opposite end of the pool (Fig. 3).

Turning variables were measured on the left and right hindflippers independently. There were no significant differences between data collected for the right and left hindflippers of the females (turning rate: t=0.0595, d.f.=32, P>0.05; turning radius: t=−0.390, d.f.=32, P>0.05; velocity: t=0.288, d.f.=32, P>0.05) nor of the male (turning rate: t= 0.667, d.f.=5, P>0.05; turning radius: t=−0.390, d.f.=5, P>0.05; velocity: t=0.327, d.f.=5, P>0.05). Compared with the larger male sea lion, the smaller females had faster average absolute turning rate about their hindflippers (402.8 ±96.6 deg s^{-1}) (Fig. 3), as well as a smaller average turning radius (0.40±0.09 m) (Fig. 4). With respect to the extreme 20% of the data, the females turned 31.2% faster than the male and experienced an average centripetal acceleration 240% greater than that of the male (Table 3).

Investigation into the relationships between turning variables relative to the hindflippers found strong correlations between turning rate and centripetal acceleration for females (r=0.930, n=70) and the male (r=0.852, n=15) (Fig. 5A). The equations that describe this relationship are a_c=−0.828+0.007ω for the females and a_c=−0.052+0.004ω for the male. The slopes of this relationship differed significantly (t=5.185, d.f.=81, P<0.001). A significant correlation was also found between velocity and centripetal acceleration for the females (r=0.844, P<0.01, n=70) and the male (r=0.629, P<0.05, n=15) (Fig. 5B). These relationships are described by the equations a_c=−1.819+1.404**U** for females and a_c=−0.256+0.555**U** for the male. The slopes of this relationship were significantly different (t=3.877, d.f.=81, P<0.001).

The mean angle of attack of the hindflippers through the banking turn was 28.6±7.4 deg for the females and 26.8±7.5 deg for the male (Fig. 6). There was no significant difference in the angle of attack of the hindflippers between the female and male sea lions (t= 0.937, d.f.=22, P>0.05). Thus, the data were pooled and the average angle of attack of the hindflippers from the combined data was 28.3±7.3 deg. In the extreme 20% of the data, the average angle of attack was 8–12 deg greater than the pooled average and the maximum angle of attack was 48.5 and 50.8 deg for the male and females, respectively (Table 3). The average spread angle of the abducted hindflippers from five adult specimens was 30.2±3.1 deg.

Journal of Experimental Biology (2021) 224, jeb243020. doi:10.1242/jeb.243020

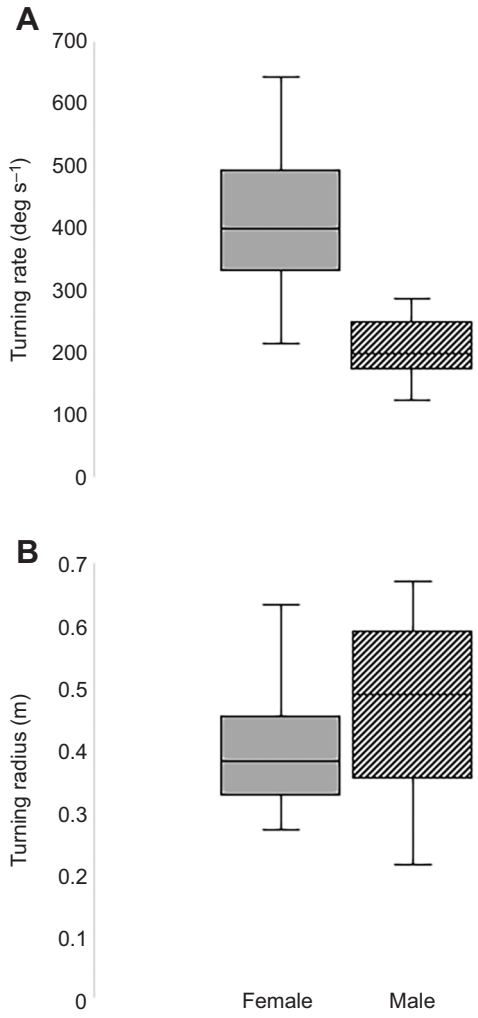

Fig. 4. Turning rate and turning radius calculated about the hindflippers for 3 captive California sea lions. (A) Turning rate and (B) turning radius data for 2 female and 1 male sea lion are averages and 95% confidence intervals. Turns analyzed about the right hindflipper: females *n*=33, male *n*=9; turns analyzed about the left hindflipper: females *n*=37, male *n*=6.

DISCUSSION

Porpoising

Porpoising is a behavior typically performed at high swimming speeds (Au et al., 1988; Au and Weihs, 1980). The critical speed at which an animal transitions from swimming to porpoising occurs when the energy used to leap is lower than the energy required to swim just below the water surface. This critical speed varies among marine animals, but is typically around 3.0–3.5 m s^{-1} (Hui, 1987; Au et al., 1988). The 2.13±0.26 m s^{-1} average exit velocity (Table 2) of the porpoising sea lion from the National Zoo may be assumed to represent the average critical speed of this individual. This speed coincides with the predicted porpoising speed for a dolphin of similar body length (Blake, 1983; Fish and Rohr, 1999). While sufficient to leap, the average exit speed of this captive sea lion is lower than the expected critical speed for porpoising (Blake and Smith, 1988). The low exit speeds of the sea lion were sufficient to leap, where the leaps were vertically exaggerated compared with those of sea lions in the wild. It may be that in the wild the exit angle is low to maintain a fast speed without losing momentum, but allow sufficient time in the aerial phase for breathing (Hui, 1987; 1989). While models predict that porpoising could conserve swimming energy at slower swimming speeds, the leaping analyzed from the captive animal in the present study is thought to be too small to increase efficiency (Blake and Smith, 1988). The slower porpoising analyzed in the captive environment is likely due to the differing motivations behind wild and captive porpoising – the motivation here being a training command and the presence of food.

In the wild, animals typically porpoise as a survival/energy conservation strategy (Kooyman, 1975; Wilson, 1995; Yoda et al., 1999). For example, wild penguins tend to porpoise only at the beginning and end of a foraging trip, or when startled as related to escape behaviors (Randall and Randall, 1990; Yoda et al., 1999). Penguin predators, such as sharks, leopard seals and killer whales, will often congregate in the waters near penguin nesting sites, prepared to ambush the penguins as they travel to and from shore (Wilson, 1995). Porpoising is believed to allow penguins the ability to ventilate while maintaining speed and escaping predators (Hui, 1987; Blake and Smith, 1988; Yoda et al., 1999). Sea lions share a semi-aquatic lifestyle with penguins and are preyed upon by a number of the same predators. The advantages in transport and ventilation that porpoising provides to penguins likely also benefit wild sea lions (Boness, 2009).

Studies on dolphin porpoising have found that during the submerged portion of porpoising, dolphins execute two different swimming phases: (1) coast swimming, where the animal stabilizes and decelerates, and (2) burst swimming, where the animal accelerates back up to speed prior to the next leap (Weihs, 2002). Thus, dolphins swim underwater for twice the length of their leap before repeating the cycle (Au et al., 1988). The sea lion subject of this study was trained to porpoise in front of the exhibit viewing window, thereby restricting her to two leaps before needing to complete a 180 deg turn to continue the porpoising bout. Trainers expected the sea lion to continue rapid leaping until they recalled the animal for a reward, and this may have affected the measured variables. The constraints of the captive environment may have resulted in a slower and more horizontally compressed porpoising behavior than would be witnessed out in the wild. Similarly, the sea lion's mean angle upon leaving the water was 70.0±6.3 deg (Table 2), which was nearly 1.6 times greater than that of the wild porpoising sea lions and nearly 1.8 times greater than the average exit angle of porpoising dolphins (Weihs, 2002). Dolphins exit the water at an angle of 39 deg, which is a compromise between the angle of optimal leap length (45 deg) and the angle of optimal horizontal speed (30 deg) (Weihs, 2002). Animals porpoising in the wild seek to maximize distance, speed and efficiency (Kooyman, 1975; Hui, 1987; Blake and Smith, 1988; Au et al., 1988; Wilson, 1995; Yoda et al., 1999; Weihs, 2002), while the captive sea lion displayed an amplified height as a result of its training. However, wild sea lions exited the water at exactly 45 deg, indicating an optimal leap length to maintain a rapid transient swimming speed.

Turning

There is a stark difference in the mechanics and performance of turning animals in relation to the flexibility of the body (Webb, 1975; Fish, 2002; Walker, 2000). Animals with a highly rigid body structure, namely in the axial body, such as sea turtles (Superfamily: Chelonioidea) or the whirligig beetle (*Dineutus horti*) typically perform powered turns and utilize asynchronous movements of the limbs to complete turns (Davenport and Clough, 1986; Renous and Bels, 1993; Fish and Nicastro, 2003; Fish, 2004; Rivera et al., 2006). Whirligig beetles exhibit an impressive maximum turning rate of 4428 deg s^{-1}, which is largely a function of their small size,

Journal of Experimental Biology (2021) 224, jeb243020. doi:10.1242/jeb.243020

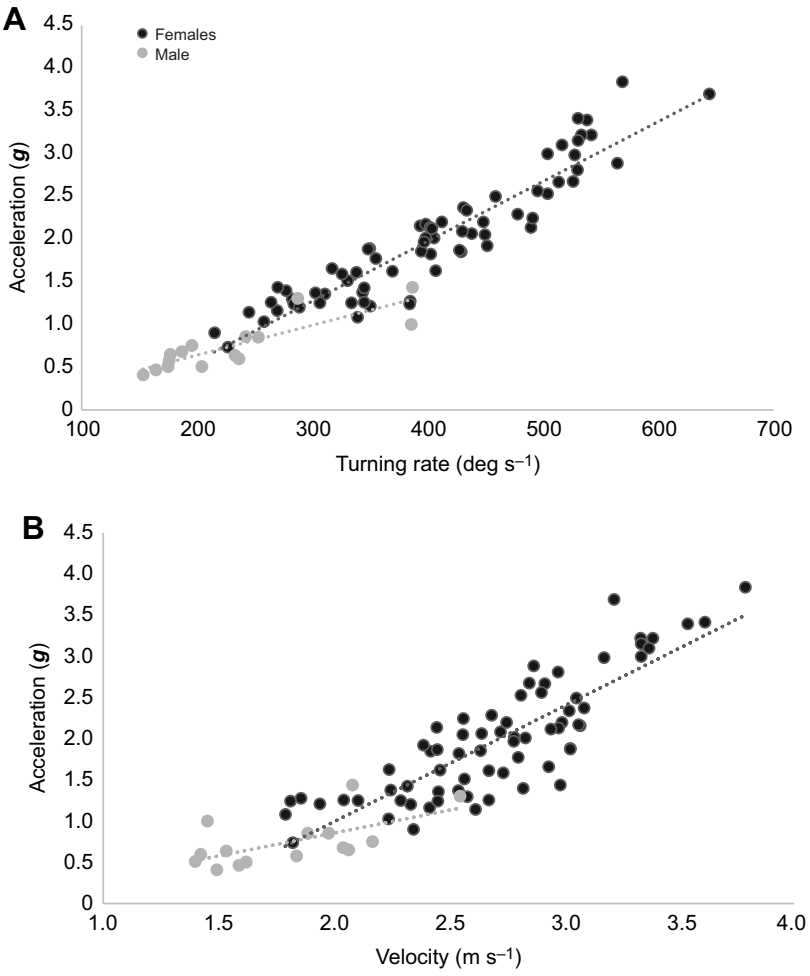

Fig. 5. Relationship between centripetal acceleration with respect to gravitational acceleration (*g*) and turning rate and turning velocity about the hindflippers among 3 captive California sea lions. (A) Turning rate and (B) turning velocity data for 2 female and 1 male sea lion.

as turning rate is inversely proportional to body length (Fish and Nicastro, 2003). The turning rates of larger rigid bodied aquatic organisms better exemplify the restrictions that stiffness places on turning performance. For example, various species of rays can only turn at a maximum of 30.4 or 44.4 deg s^{-1} depending on their swimming mode (i.e. undulatory or oscillatory movements) (Parson et al., 2011). The rigid mantle of squid restricts their maximum turning rate to 90 deg s^{-1} (Foyle and O'Dor, 1988). The turning rate of the spotted boxfish (*Ostracion meleagris*) is 218 deg s^{-1}, though this comes at the expense of a greater turning radius (Walker, 2000). Of the rigid bodied aquatic animals, Humboldt penguins (*Spheniscus humboldti*) have notable turning performance, completing powered turns with a turn radius of approximately 25% of their body length and an average turning rate of 232 deg s^{-1} (Hui, 1985). Penguins, like sea lions, swim by pectoral propulsion. The morphology of the wings may offer penguins a greater degree of maneuverability despite their rigidity through centripetal force (Hui, 1985). Sea lions also experience centripetal force on their wing-like foreflippers during turning; however, *Z. californianus* greatly out maneuvers penguins with the aid of their flexibility and behavioral techniques (Fish et al., 2003; Fish, 2004).

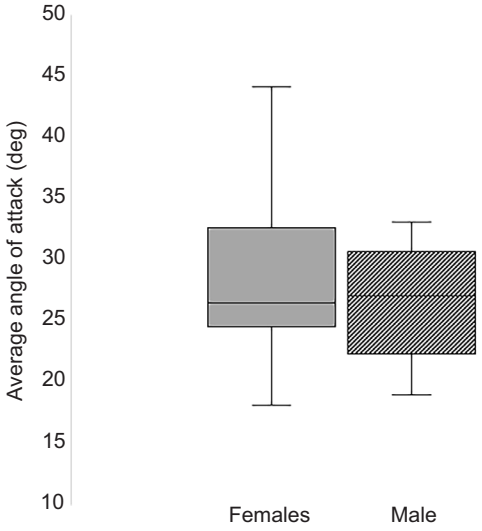

Fig. 6. Angle of attack of the hindflippers during bank turning maneuvers for 3 captive California sea lions. Data are averages and 95% confidence intervals for 2 female and 1 male sea lion. Individual turns analyzed: females *n*=58 and male *n*=12.

An increase of flexibility in the axial body allows animals to more easily complete turns with a small turn radius at a high turn rate (Fish, 2002; Fish and Nicastro, 2003). Cetaceans (whales, dolphins and porpoises) are considered to have moderate axial flexibility and are known to utilize behavioral techniques (e.g. unpowered turns, banking), all of which provide benefits to maximum turning performance. Cetaceans execute unpowered turns to take advantage of large lift forces and small turn radii of 11–17% of body length (Fish, 2002; Blake and Chan, 2006). Some cetaceans, such as the

Journal of Experimental Biology (2021) 224, jeb243020. doi:10.1242/jeb.243020

blue whale (*Balaenoptera musculus*), include a 15–90 deg roll of the body (i.e. banking) in their unpowered turns to further exploit dorsoventral flexibility and improve their turning performance (Segre et al., 2019). Generally, cetaceans complete small radius turns at turn rates of up to 200 deg s^{-1}. However, Pacific white-sided dolphins (*Lagenorhynchus obliquidens*) were found to perform unpowered turns with a maximum turning rate of 453 deg s^{-1} (Fish, 2002).

The sea lion has tremendous axial flexibility, which allows this pinniped to be highly maneuverable (Fish, 2002; Fish et al., 2003). *Zalophus californianus* performs subaqueous turns by utilizing its foreflippers and abducted hindflippers in unpowered turns with a 90 deg banking body roll (Fish et al., 2003; Fish, 2004). The location of the control surfaces (i.e. flippers) and flexibility of the body make the basic body design unstable (Fish, 2002). With the placement of the foreflippers close to the center of mass, they are unlikely to be solely responsible for producing the forces necessary for *Z. californianus* to complete rapid, tight turns (Fish et al., 2003). However, sea lions also utilize the large area of their abducted, delta-shaped hindflippers while turning. As a result, the sea lion demonstrates superior turning performance compared with moderately stable-bodied cetaceans with respect to both turning radius and turning rate (Fish, 2002; 2004; Fish et al., 2003). With respect to the center of gravity, sea lions were previously found to complete banked turns with a maximum turning rate of 690 deg s^{-1} and a minimum turning radius of less than 10% of body length (Fish et al., 2003). Fish et al. (2003) determined that sea lions executing turns at these high rates and small radii would experience centripetal accelerations of up to 5.13 ***g***.

Turns in the present study were not analyzed about the center of gravity, but instead with respect to the hindflippers. With the exception of length-specific turning radius (Table 3), the smaller female sea lions in this study outperformed the male, including an average turning rate of 540.7±34.6 deg s^{-1} versus the male's 353.2 ±57.0 deg s^{-1}. Compared with those previously determined values for maximum turning performance of sea lions, the banking turns analyzed in this study likely represent 'moderate' turning performance. In the extreme 20% of the data for females, the mean centripetal acceleration at the hindflippers was approximately 2 ***g*** slower than what has been reported for maximal performance about the center of gravity (Table 3) (Fish et al., 2003). It was considered that the sea lions in this experiment were not pushed to their maximum turning performance as that was not the focus of this study and the small size of the experimental pool restricted the velocity at which the sea lions could perform the 180 deg turn. However, it is likely that the mechanics/angle of attack of the hindflippers in this study was representative of the performance of wild sea lions during routine foraging, which would likely be further exaggerated during bouts of maximum performance.

Hindflippers as control surfaces

In aerodynamics, a typical, unmodified, straight wing will experience stall with a dramatic loss of lift at an angle of attack around 11–12 deg (Miklosovic et al., 2004), whereas delta-wings continue producing lift and delay stall beyond 30 deg (Katz and Plotkin, 1991; Thompson, 1992). It is also noted that as straight wings approach the critical stall angle of attack, the craft experiences greater instabilities with regard to roll, where aircraft with swept wings (such as in a delta configuration) experience more directional instabilities about the yawing axis as they approach a stalling angle (Greer, 1972).

In biology, delta-shaped control surfaces can be found in the webbed feet and tail feathers of birds and have been proposed as structures that produce lift and delay stall in air and in water, which aids the animal in both stabilization and maneuverability (Evans, 2003; Johansson and Norberg, 2003). Evans (2003) found that during maneuvering, the tail feathers of birds function as biological delta-wings at an angle of attack less than 20 deg. The tails that exhibited a more narrow spread angle (40 deg) maintained delta-wing function at higher angles of attack than did those with a more broad spread angle (60 deg). Depending on the species, the lift generated by the static delta tail surface was enough to support 11–73% of the bird's body weight in flight (Evans, 2003). Analogous to the tail feathers of birds, sea lions use their hindflippers as static rather than propulsive control surfaces. The sea lions abduct the digits of the hindflippers to a spread angle of about 30 deg to increase the surface area of these surfaces and then maintain this posture throughout the aquatic maneuver. The delta-shape of the abducted hindflippers stabilizes the hind-region throughout the maneuver and potentially generates lift to reduce turn radius.

It is difficult to establish an operational range of angles at which a biological control surface may be considered a delta-wing as the location of the control surface, shape of the animal's body and the action of the control surface all affect lift properties (Evans, 2003; Johansson and Norberg, 2003). Based on the aerodynamics of straight wings stalling around 11–12 deg (Miklosovic et al., 2004) and delta wings maintaining lift and delaying stall well above 12 deg (Katz and Plotkin, 1991; Thompson, 1992), we estimated that delta-shaped control surfaces beneficially operate as biological delta-wings at angles of attack greater than 12 deg.

During porpoising, the abducted hindflippers stabilize the hind-region upon water entry and are then held at an average angle of attack of 14.6±6.3 deg with a range of 10.8–18.3 deg (Table 2) through the submerged lift-producing phase of the leap. While the minimum of angle of attack range falls below the proposed

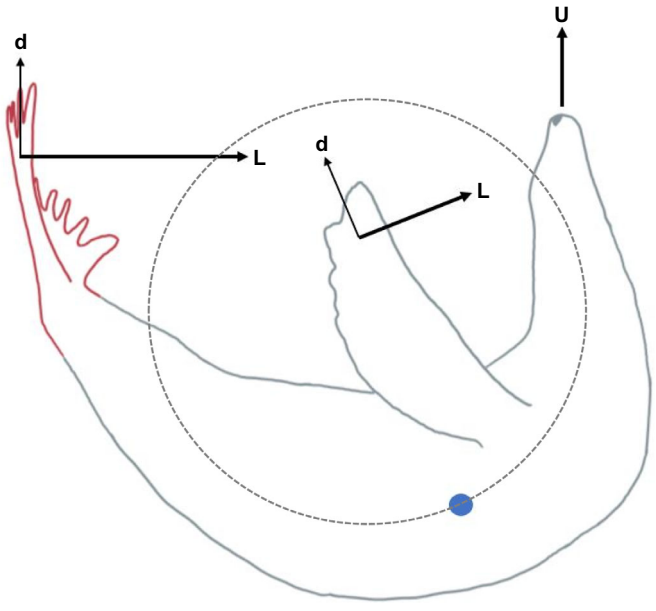

Fig. 7. Proposed force vectors acting on the control surfaces (i.e. foreflippers and hindflippers) of a California sea lion during a left banking turn. The red outline highlights the hindflippers and the blue circle represents the location of the center of mass. The forces depicted are lift (**L**) and drag (**d**) acting on the control surfaces, and velocity (**U**).

minimum for biological delta-wing function of 12 deg, 80% of the measured values were greater than 12 deg. While turning underwater, the average angle of attack of the hindflippers increased for both male (26.8±7.5 deg) and female (28.6±7.4 deg) sea lions (Fig. 6). These angles occupied the upper end of the known operational range of true delta-wings, let alone biological delta-wings. Despite the high angle of attack of the hindflippers, the flippers themselves as well as the hind-region of the body remained stable along the curved trajectory of the turn and did not display any instabilities characteristic of a stalling wing (Greer, 1972), providing further support for delta-wing function. It is also possible that sea lions may further increase the angle of attack of their hindflippers to accomplish their maximum performance during subaqueous behaviors.

At no point during either porpoising or turning trials did the animals complete these behaviors with adducted hindflippers. The full span of the delta-shaped hindflippers was consistently deployed, providing a large aquatic control surface for lift generation throughout the high-performance maneuvers (Fig. 7). The hindflippers' position far from the center of gravity, characteristic triangular shape and operation at high angles of attack during porpoising and turning maneuvers without evidence of stalling instabilities indicate these control surfaces function as biological delta-wings. These findings provide further insight into lift-based aquatic maneuverability and may be implemented in future bioinspired designs of aquatic vehicles to increase turning performance.

Acknowledgements
We wish to express our gratitude to the sea lion staff at SLEWTHS and the National Zoo for their dedication to training the sea lions to accommodate this study. Our thanks are also extended to Dr Alison Kolpas for use of her custom-written Matlab code for turning analyses.

Competing interests
The authors declare no competing or financial interests.

Author contributions
Conceptualization: A.M.L.; Methodology: J.A.Z., S.S.; Formal analysis: A.M.L.; Investigation: A.M.L., S.J.K., K.L.C.; Resources: F.E.F., J.A.Z., S.S.; Data curation: A.M.L.; Writing - original draft: A.M.L.; Writing - review & editing: F.E.F.; Visualization: A.M.L.; Supervision: F.E.F.; Project administration: F.E.F., M.L.; Funding acquisition: F.E.F., M.L.

Funding
This research was supported by grants from the Office of Naval Research (N000141712312, program manager Thomas McKenna) to M.C.L.

Data availability
The data that support the findings of this study are openly available from the Dryad digital repository (Leahy, 2021): https://doi.org/10.5061/dryad.0p2ngf21s

References
Au, D. and Weihs, D. (1980). At high speeds dolphins save energy by leaping. *Nature* **284**, 548-550. doi:10.1038/284548a0
Au, D. W., Scott, M. D. and Perryman, W. L. (1988). Leap-swim behavior of "porpoising" dolphins. *Cetus* **8**, 7-10.
Blake, R. W. (1983). Energetics of leaping in dolphins and other aquatic animals. *J. Mar. Biolog. Assoc. UK* **6**, 61-67. doi:10.1017/S0025315400049808
Blake, R. W. and Chan, K. H. S. (2006). Models of the turning and fast-start swimming dynamics of aquatic vertebrates. *J. Fish Biol.* **69**, 1824-1836. doi:10.1111/j.1095-8649.2006.01251.x
Blake, R. W. and Smith, M. D. (1988). On penguin porpoising. *Can. J. Zool.* **66**, 2093-2094. doi:10.1139/z88-310
Boness, D. J. (2009). Sea lions: overview. In *Encyclopedia of Marine Mammals*, 2nd edn (ed. W. F. Perrin, B. Würsig and J. G. M. Thewissen) pp. 998-1001. Cambridge, MA: Academic Press.
Davenport, J. and Clough, W. (1986). Swimming and diving in young logger-head sea turtles (*Caretta caretta L.*). *Copeia* **1986**, 53-57. doi:10.2307/1444887
Di Stefano, J. (2004). A confidence interval approach to data analysis. *For. Ecol. Manag.* **187**, 173-183.
English, A. W. M. (1976). Limb movements and locomotor function in the California sea lion (*Zalophus californianus*). *J. Zool. Lond.* **178**, 341-364. doi:10.1111/j.1469-7998.1976.tb02274.x
Evans, M. R. (2003). Bird's tails do act like delta wings but delta-wing theory does not always predict the forces they generate. *Proc. R. Soc. Lond.* **270**, 1379-1385. doi:10.1098/rspb.2003.2373
Feldkamp, S. D. (1987a). Foreflipper propulsion in the California sea lion, *Zalophus californianus*. *J. Zool. Lond.* **212**, 43-57. doi:10.1111/j.1469-7998.1987.tb05113.x
Feldkamp, S. D. (1987b). Swimming in the California sea lion: morphometrics, drag, and energetics. *J. Exp. Biol.* **131**, 117-135. doi:10.1242/jeb.131.1.117
Fish, F. E. (2002). Balancing requirements for stability and maneuverability in cetaceans. *Integr. Comp. Biol.* **42**, 85-93. doi:10.1093/icb/42.1.85
Fish, F. E. (2004). Structure and mechanics of non-piscine control surfaces. *IEEE J. Ocean. Eng.* **29**, 605-621. doi:10.1109/JOE.2004.833213
Fish, F. E., Innes, S. and Ronald, K. (1988). Kinematics and estimated thrust production of swimming harp and ringed seals. *J. Exp. Biol.* **137**, 157-173. doi:10.1242/jeb.137.1.157
Fish, F. E. and Hui, C. A. (1991). Dolphin swimming- a review. *Mammal. Rev.* **21**, 181-195. doi:10.1111/j.1365-2907.1991.tb00292.x
Fish, F. E. and Rohr, J. (1999). *Review of dolphin hydrodynamics and swimming performance*. SPAWARS System Center Technical Report 1801, San Diego, CA.
Fish, F. E., Hurley, J. and Costa, D. P. (2003). Maneuverability by the sea lion *Zalophus californianus*: turning performance of an unstable body design. *J. Exp. Biol.* **206**, 667-674. doi:10.1242/jeb.00144
Fish, F. E. and Nicastro, A. J. (2003). Aquatic turning performance by the whirligig beetle: constraints on maneuverability by a rigid biological system. *J. Exp. Biol.* **206**, 1649-1656. doi:10.1242/jeb.00305
Fish, F. E. and Lauder, G. V. (2017). Control surfaces of aquatic vertebrates in relation to swimming modes. *J. Exp. Biol.* **220**, 4351-4363. doi:10.1242/jeb.149617
Foyle, T. P. and O'Dor, R. K. (1988). Predatory strategies of squid (*Illex illecebrosus*) attacking small and large fish. *Mar. Freshw. Behav. Physiol.* **13**, 155-168. doi:10.1080/10236248809378670
Friedman, C. and Leftwich, M. C. (2014). The kinematics of the California sea lion foreflipper during forward swimming. *Bioinspir. Biomim.* **9**, 046010. doi:10.1088/1748-3182/9/4/046010
Godfrey, S. J. (1985). Additional observations of subaqueous locomotion in the California Sea Lion (*Zalophus californianus*). *Aquat. Mamm.* **11**, 53-57.
Gordon, K. R. (1983). Mechanics of the limbs of the walrus (*Odobenus rosmarsus*) and the California sea lion (*Zalophus californianus*). *J. Morphol.* **175**, 73-90. doi:10.1002/jmor.1051750108
Greer, D. H. (1972). Summary of directional divergence characteristics of several high-performance aircraft configurations. *NASA Technical Note* D-6993.
Hamizi, I. B. and Khan, S. A. (2019). Aerodynamics investigation of delta wing at low Reynold's number. *CFD Letters* **11**, 32-41.
Hui, C. A. (1985). Maneuverability of the Humboldt penguin (*Spheniscus humboldti*) during swimming. *Can. J. Zool.* **63**, 2165-2167. doi:10.1139/z85-318
Hui, C. A. (1987). The porpoising of penguins: an energy-conserving behavior for respiratory ventilation? *Can. J. Zool.* **65**, 209-211. doi:10.1139/z87-031
Hui, C. A. (1989). Surfacing behavior and ventilation in free-ranging dolphins. *J. Mammal.* **70**. 833-835. doi:10.2307/1381722
Johansson, L. C. and Norberg, R. A. (2003). Delta-wing function of webbed feet gives hydrodynamic lift for swimming propulsion in birds. *Nature* **424**, 65-68. doi:10.1038/nature01695
Katz, J. and Plotkin, A. (1991). *Low-Speed Aerodynamics*. New York: McGraw-Hill.
Kooyman, G. L. (1975). Behavior and physiology of diving. In *The Biology of Penguins* (ed. B. Stonehouse), pp. 115-138. London, UK: Macmillan.
Leahy, A. (2021). Zalophus hindflipper turning metrics and angle of attack. *Dryad, Dataset.* doi:10.5061/dryad.0p2ngf21s
Marchman, J. F. (1981). Effectiveness of leading-edge vortex flaps on 60 and 75 degree delta wings. *J. Aircr.* **18**, 280-286. doi:10.2514/3.44702
Miklosovic, D. S., Murray, M. M., Howle, L. E. and Fish, F. E. (2004). Leading edge tubercles delay stall on humpback whale (*Megaptera novaeangliae*) flippers. *Phys. Fluids* **16**, L39-L42. doi:10.1063/1.1688341
Parson, J. M., Fish, F. E. and Nicastro, A. J. (2011). Turning performance of batoids: limitations of a rigid body. *J. Exp. Mar. Biol. Ecol.* **402**, 12-18. doi:10.1016/j.jembe.2011.03.010
Polhamus, E. C. (1966). A concept of the vortex lift of sharp-edge delta wings based on a leading-edge-suction analogy. *NASA Technical Note* D-3767.
Pugliares, K. R., Bogomolni, K. M. A., Touhey, S. M., Herzig, C. T., Harry, and Moore, M. J. (2007). *Marine mammal necropsy: an introductory guide for stranding responders and field biologists*. Woods Hole Oceanographic Institution Technical Report WHOI-2007-06. Woods Hole, MA.
Randall, R. M. and Randall, B. M. (1990). Cetaceans as predators of Jackass penguins *Spheniscus demersus*: deductions based on behaviour. *Mar. Ornithol.* **18**, 9-12.

Renous, S. and Bels, V. (1993). Comparison between aquatic and terrestrial locomotions of the leatherback sea turtle (*Dermochelys coriacea*). *J. Zool. Zool. Soc. Lond.* **230**, 357-378. doi:10.1111/j.1469-7998.1993.tb02689.x

Rivera, G., Rivera, A. R. V., Doughtry, E. E. and Blob, R. W. (2006). Aquatic turning performance of painted turtles (*Chrysemys picta*) and functional consequences of a rigid body design. *J. Exp. Biol.* **209**, 4203-4213. doi:10.1242/jeb.02488

Rom, J. (1992). *High Angle of Attack Aerodynamics: Subsonic, Transonic, and Supersonic Flow*. New York: Springer.

Segre, P. S., Cade, D. E., Calambokidis, J., Fish, F. E., Friedlaender, A. S., Potvin, J. and Goldbogen, J. A. (2019). Body flexibility enhances maneuverability in the world's largest predator. *Integr. Comp. Biol.* **59**, 48-60. doi:10.1093/icb/icy121

Tarasoff, F. J. (1972). Comparative aspects of the hind limbs of the river otter, sea otter, and seals. In *Functional Anatomy of Marine Mammals* (ed. R. J. Harrison), pp. 333-359. New York: Academic Press.

Thompson, S. A. (1992). The unsteady aerodynamics of a delta wing undergoing large amplitude pitching motions. *PhD thesis*, University of Notre Dame, Notre Dame, IN, USA.

Walker, J. A. (2000). Does a rigid body limit maneuverability? *J. Exp. Biol.* **203**, 3391-3396. doi:10.1242/jeb.203.22.3391

Webb, P. W. (1975). Hydrodynamics and energetics of fish propulsion. *Bull. Fish. Res. Board Can.* **190**, 1-158.

Weihs, D. (2002). Dynamics of dolphin porpoising revisited. *Integr. Comp. Biol.* **42**, 1071-1078. doi:10.1093/icb/42.5.1071

Whitlock, W. C. and Schluter, D. (2015). *The Analysis of Biological Data*, 2nd edn. New York: W.H. Freeman and Company.

Williams, T. M. (2001). Intermittent swimming by mammals: a strategy for increasing energetic efficiency during diving. *Am. Zool.* **41**, 166-176.

Williams, T. M., Davis, R. W., Fuiman, L. A., Francis, J., Le, B. J., Horning, M., Calambokidis, J. and Croll, D. A. (2000). Sink or swim: strategies for cost-efficient diving by marine mammals. *Science* **288**, 133-136. doi:10.1126/science.288.5463.133

Wilson, R. P. (1995). Foraging ecology. In *The Penguins* (ed. T. D. Williams), pp. 81-106. Oxford: Oxford University Press.

Yoda, K., Sato, K., Niizuma, Y., Kurta, M., Bost, A., Le Maho, Y. and Naito, Y. (1999). Precise monitoring of porpoising behaviour of Adelie penguins determined using acceleration data logs. *J. Exp. Biol.* **202**, 3121-3126. doi:10.1242/jeb.202.22.3121